

Free flight maneuvers of stalk-eyed flies: do eye-stalks affect aerial turning behavior?

Gal Ribak · John G. Swallow

Received: 6 March 2007 / Revised: 26 July 2007 / Accepted: 27 July 2007 / Published online: 21 August 2007
© Springer-Verlag 2007

Abstract The eyes of stalk-eyed flies (Diopsidae) are positioned at the end of rigid peduncles projected laterally from the head. In dimorphic species the eye-stalks of males exceed the eye-stalks of females and can exceed body length. Eye-stalk length is sexually selected in males improving male reproductive success. We tested whether the long eye-stalks have a negative effect on free-flight and aerial turning behavior by analyzing the morphology and free-flight trajectories of male and female *Cyrtodiopsis dalmanni*. At flight posture the mass-moment-of-inertia for rotation about a vertical axis was 1.49-fold higher in males. Males also showed a 5% increase in wing length compared to females. During free-flight females made larger turns than males (54 ± 31.4 vs. $49 \pm 36.2^\circ$, *t* test, $P < 0.033$) and flew faster while turning (9.4 ± 5.45 vs. 8.4 ± 6.17 cm s⁻¹, ANOVA, $P < 0.021$). However, turning performance of both sexes overlapped, and turn rate in males even marginally exceeded turn rate in females (733 ± 235.3 vs. 685 ± 282.6 deg s⁻¹, ANCOVA, $P < 0.047$). We suggest that the increase in eye-span does result in an increase in the mechanical requirements for aerial turning but that male *C. dalmanni* are capable of compensating for the constraint of longer eye-stalks during the range of turns observed through wingbeat kinematics and increased wing size.

Keywords Maneuverability · Saccade · Free-flight · Diopsidae · Moment-of-inertia

Abbreviations

MOI Moment of inertia

Introduction

During flight within large enclosures flies typically engage in rapid directional changes separated by intervals of relatively straight flight (Land and Collett 1974; Collett and Land 1975; Wagner 1986; Tammero and Dickinson 2002a). The abrupt changes in flight direction are believed to function similarly to saccadic eye motions in humans (Land 1999). By performing rapid directional adjustments (“saccadic” turns) interspaced by periods of straight flight, flies minimize the duration of blurred image on the retina when the fixed eye rotates with the head and body (Land and Collett 1974). Vision plays a major role in the initiation of turning behavior (Heisenberg and Wolf 1979; Götz and Wandel 1984; Wagner 1986; Mayer et al. 1988; Tammero and Dickinson 2002a; Frye et al. 2003; Bender and Dickinson 2006a), but other sensory organs such as the halteres probably take over the control of turning dynamics within the maneuver once initiated (Tammero and Dickinson 2002b; Bender and Dickinson 2006b). The turns are produced by asymmetric wing-beats between the left and right wings as the flies, over several wing beats, power both the initiation and termination of the saccade (Heide and Götz 1996; Frye et al. 2003; Dickinson 2005). Both the resistance of air and inertia of the body determine how a net torque developed by the wings will be expressed as rotation dynamics of the fly during flight (Frye et al. 2003). Therefore, rapid turns such as saccades may be limited by the angular velocity in which a fly can rotate its body in air.

G. Ribak (✉) · J. G. Swallow
Department of Biology,
University of South Dakota,
Vermillion, SD 57069, USA
e-mail: gribak@usd.edu

Stalk-eyed flies (diopsidae) have eyes placed laterally away from the head on elongated peduncles (Shillito 1971). Within the family, both males and females share this morphological characteristic, but in some of the species eye-stalk length is sexually dimorphic with the distance between the left and right eye (“eye span”) in males exceeding the eye span of females (Wilkinson and Dobson 1997). In dimorphic species, such as *Cyrtodiopsis dalmanni* (Fig. 1), lateral growth of the eye-stalks in males can result in an eye span that considerably exceeds body length (Baker and Wilkinson 2001). Studies have shown that in dimorphic species eye-stalk length in males is a sexually selected trait. Female mate choice favors males with longer eye-stalks (Burkhardt and De la Motte 1988; Wilkinson and Reillo 1994; Wilkinson et al. 1998) and males with smaller eye span retreat faster from confrontations with larger males when competing in terrestrial territorial fights over access to roosting sites where females come to mate (Panhuis and Wilkinson 1999). As an emerging model organism for evolution by sexual selection, there is a growing literature on the development and expression of eye-stalks (David et al. 2000; Cotton et al. 2004), eye-stalk allometry (Wilkinson 1993; Knell et al. 1999; Baker and Wilkinson 2001), reproductive behavior (Alighali 1984; Wilkinson et al. 1998), reproductive isolation (Christianson et al. 2005; Swallow et al. 2005) and population genetics (Wilkinson et al. 2003; Wright et al. 2004) of stalk-eyed flies. However, the consequences of eye-stalk elaboration outside of the context of mate competition has rarely been addressed.

Because the laterally protruding eyes seem like an inefficient arrangement for flight, trade-offs between these secondary sexual traits and aerial performance might be expected. Swallow et al. (2000) compared the flight speeds and the variation in flight direction between two closely related stalk-eyed flies: *Cyrtodiopsis whitei*, a species with long eye-stalks and large differences in eye span between males and females (mean eye span ♀ = 6.5, ♂ = 9.8 mm) and *C. quinqueguttata*, a monomorphic species with short eye-stalks (♀ = 4.06, ♂ = 4.40 mm; Table 1 in Swallow et al. 2000). Two findings from that study that are of concern here were that: (1) after correcting for differences in body mass, head mass did not differ between the sexes or species (adjusted mean of head mass *C. quinqueguttata*: ♀ = 0.79 ± 0.04 , ♂ = 0.81 ± 0.02 , *C. whitei* ♀ = 0.80 ± 0.02 , ♂ = 0.84 ± 0.03 mg), and (2) the males of *C. whitei* (long eye-stalks) showed a slight ($P = 0.047$) tendency to maintain flight direction within a narrower range of variability than the *C. quinqueguttata* males or the females from both species. That study suggested differences in visual processing, drag of the eyes, or aerodynamic interference in the wake of the eye-stalks as possible mechanisms for the observed

differences in flight velocity and straightness (Swallow et al. 2000).

An additional explanation for the straightness of flight in males with longer eye-stalks may involve the associated change in distribution of mass along the lateral axis. Rotating a rigid object about a given axis requires a net moment (torque). The relation between the magnitude of the moment and the resulting angular acceleration of the object (neglecting air resistance) is the mass moment of inertia (MOI) which is specific for the axis of rotation. MOI is inversely related to the responsiveness of an object to torques and depends on mass (m) and its distance from the axis of rotation (R) raised to the second power ($\text{MOI} = mR^2$; Fox 1967). The compound eyes of flies are large organs (Zeil 1983). The dependence of MOI on the second power of distance indicates that small changes in lateral displacement of the eye (eye span) can have a large effect on the MOI of the body. Dudley (2002) pointed out that explaining the agility and maneuverability of animal flight, requires consideration of not only the power output of the wings but also the responsiveness of the body segments to rotations and translations. How stalk-eyed flies fall within these limitations and to what extent their turning behavior is affected by the unique shape of the head has never been studied to the best of our knowledge.

The objectives of this study were (1) to evaluate the effect of eye-stalk elongation on the MOI of the body, (2) to provide a description of the aerial turning behavior of stalk-eyed flies during free flight, and (3) to compare the turning performance between females and males stalk-eyed flies that differ considerably in eye span. The morphology and distribution of mass along body axes were evaluated using measurements on dead flies. Additionally, we tracked the free flight trajectories of female and male *C. dalmanni* within a large flight chamber and analyzed the turns displayed by both sexes to assess the effect of head dimorphism on aerial turning.

Methods

Flies

Male and female *C. dalmanni* used in the experiment were obtained as pupae from a large population reared at the University of Maryland at College Park. After eclosing the flies were kept in clear, 16 l, plastic containers, at a temperature of 26°C and a light:dark cycle of 12:12 h. The containers were bedded with moist cotton. The flies had access to water and food (mashed corn) *ad libitum*. In *C. dalmanni* sexual maturity is achieved after 1 week and peaks at 4 weeks from eclosion (Reguera et al. 2004). Because evidence indicated that body mass increases for

Table 1 Mean ± SD of morphological measurements from male and female *C. dalmanni*

Measurement	♂	♀	Significance test
Mass (mg)			
Total body	7.12 ± 1.033	6.83 ± 1.034	$t_{38} = -0.89$
Eyes	0.24 ± 0.053	0.25 ± 0.048	$F_{1,37} = 0.04$
Eye-stalks	0.11 ± 0.031	0.07 ± 0.020	$F_{1,37} = 19.94^{***}$
Head – (Eyes + Stalks)	0.27 ± 0.070	0.28 ± 0.062	$F_{1,37} = 3.57$
Total head	0.63 ± 0.135	0.59 ± 0.111	$F_{1,37} = 0.11$
Thorax	2.89 ± 0.406	2.26 ± 0.509	$F_{1,37} = 4.30^*$
Abdomen	1.98 ± 0.566	2.37 ± 0.624	$F_{1,37} = 30.3^{***}$
Front legs	0.65 ± 0.125	0.43 ± 0.095	$F_{1,37} = 41.5^{***}$
Size			
Eye span (mm)	8.23 ± 0.414	5.65 ± 0.264	$F_{1,37} = 655^{***}$
Wing length (mm)	4.46 ± 0.138	4.24 ± 0.138	$F_{1,37} = 56.8^{***}$
Wing area (mm ²)	4.21 ± 0.323	3.88 ± 0.323	$F_{1,37} = 43.3^{***}$
2nd moment area (×10 ⁻¹¹ m ⁴)	6.38 ± 0.82	5.21 ± 0.82	$F_{1,37} = 27.7^{***}$
Wing shape			
AR	9.5 ± 0.30	9.3 ± 0.53	$t_{38} = -1.48$
\hat{r}_2	0.614 ± 0.004	0.614 ± 0.003	$t_{38} = 0.45$
MOI (×10⁻¹² kg m²)			
Head (roll)	4.0 ± 0.75	1.7 ± 0.33	$t_{18} = -8.97^{***}$
Total body (roll)	5.7 ± 0.85	3.0 ± 0.49	$t_{18} = -8.39^{***}$
Head (yaw)	4.7 ± 0.95	2.1 ± 0.46	$t_{18} = -7.82^{***}$
Total body (yaw)	29.5 ± 3.68	26.6 ± 3.61	$t_{18} = -1.80$
Total body pitched at $\chi = 70^\circ$	7.6 ± 1.02	5.1 ± 0.86	$t_{18} = -6.25^{***}$

All reported averages have a sample size of 20 flies per sex except the MOI which is based on 10 flies per sex

AR is the aspect ratio of the wing, \hat{r}_2 is the non-dimensional radius of the second moment of wing area

Asterisks denote statistical significance of the difference between the sexes (* $P < 0.05$; ** $P < 0.01$; *** $P < 0.001$)

Total mass, MOI, AR and \hat{r}_2 were compared using t test. Other mass and size measurements were compared in an ANCOVA with body mass as a covariate

MOI are estimates of the moment of inertia of the head for rotations relative to the thorax and of the entire body for rotations about an axis running through the center of mass

the first 2 weeks after eclosion, we exclusively used flies 2–4 weeks post-eclosion in the experiments.

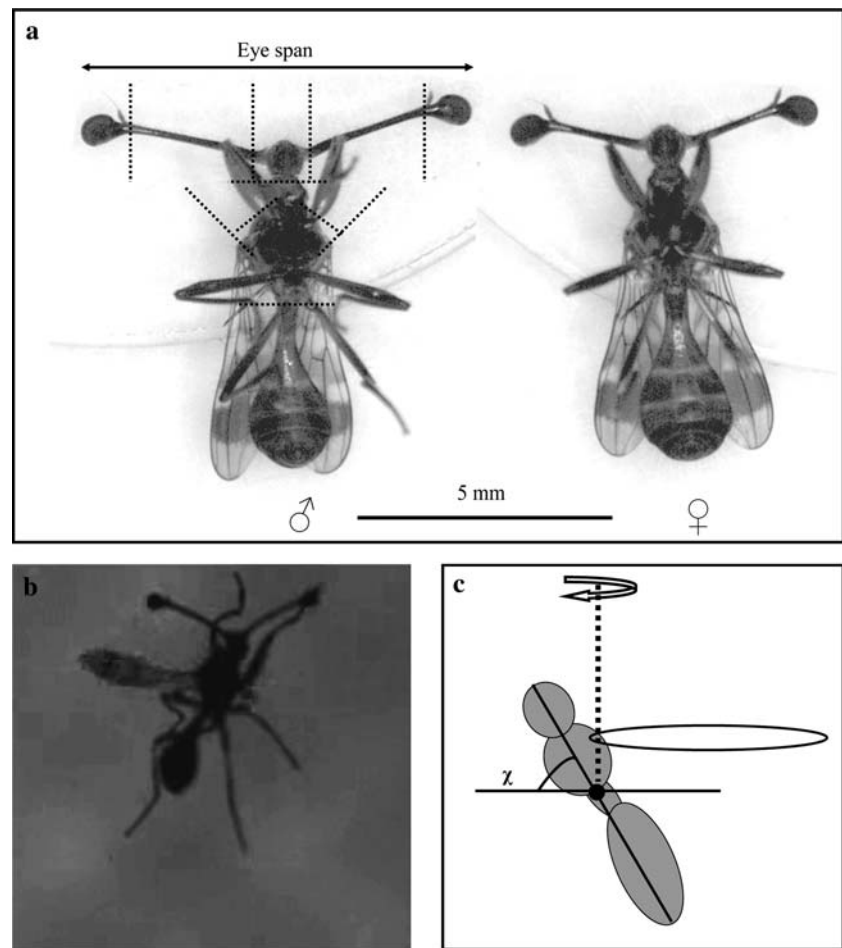
Morphological measurements

Morphological measurements were performed on 20 male and 20 female flies. Each fly was killed in chlorophorm fumes and immediately measured for body mass in a sealed pre-weighted 1.5 ml plastic tube. Mass was measured to the nearest 1 µg using an electronic microbalance (Mettler, MT5). The fly was then placed lying on its thoracic spines under a dissecting microscope connected to a digital camera. A scaled planform image of the fly was taken at magnification ×15–20 and a resolution of at least 100 pixels per mm. In the resulting images, we measured eye span as the distance between the outer edges of the two

eyes. The fly was then dissected to separate the two wings, the eyes, the eye-stalks, the remaining head, the abdomen and the anterior pair of legs leaving only the thorax and the two pair of posterior legs (Fig. 1a). The front legs of *C. dalmanni* are substantially larger than the posterior legs, and the front legs of males are substantially larger than the front legs of females (see Fig. 1a and “Results” section). Mass of all the separated body units was measured in sealed 0.3 ml test tubes to the nearest 1 µg. We evaluated mass loss during the procedure by summing the weights of all measured body units and comparing it to the initial total body mass measurement. The dissection did not exceed 5 min per fly and the measured loss was on average 12.8% (SD = 7.2, $n = 40$).

The separated wings were placed flat between a glass microscope slide and a cover glass, and a digital image was taken under magnification (×25–35). A macro program

Fig. 1 *Cyrtodiopsis dalmanni*. **a** Flies are shown lying on their upper side (ventral side opposing the camera). *Dashed lines* show the positions of transects performed to dissect the eyes, stalks, head, wings, front legs, thorax and abdomen for the morphological measurements. **b** Snapshot of a male *C. dalmanni* in flight posture viewed from a horizontal camera (vertical plane). **c** A schematic illustration describing the body angle (γ) and rotation in a horizontal plane relative to a vertical axis (*dashed line*) passing through the center of mass (*black circle*)



written for ScionImage (Scion Corp., USA) identified the wing contours from the background in the images and extracted the 2D coordinates of positions on the leading and trailing edges of the wing every 5 pixels ($\sim 22 \mu\text{m}$) along the wings major axis (length). The resulting position data were analyzed in Matlab (MathWorks Inc., USA) to calculate wing area, wing length (distance from the wing base articulation to the wing tip), aspect ratio (wing span²/wing area), the 1–3rd moments of wing area and the non dimensional radius of the second moment of wing area as in Ellington (1984).

The MOI of the body and head were estimated separately from the digital images of the flies and the weighed body sections. Using the procedure described above for wing morphology analysis, the edges of the body in the images were identified and the width of the body (left–right axis) was measured every 5 pixels along its antero-posterior axis. The width of the head (antero-posterior axis) was measured every 5 pixels along the left–right axis. Typically >100 width measurements were obtained along the major axis of the body or head. We calculated the missing dimension in the images (dorso-ventral axis) directly from the width measurements using the height-to-width ratio of the body at

each position along the body and head. The ratio was obtained for each sex from five male and five female flies that were photographed from multiple angles showing the ventral, lateral and frontal (head facing the camera) views. The measured width, height and their position on the body were divided by body length (for the body) or eye span (for the head) and interpolated (cubic-spline) so that the digitized data from all flies included the ratio of height to width at normalized fixed increments of 0.5% of the major axis. We averaged the height-to-width ratio for each position from the five flies per sex measured and used the mean ratio to calculate the dorsoventral dimension from the width in the planform images of the weighed flies. The result was the diameters of elliptical cross sections of the body (or head) measured at fixed positions along a major axis (“slices”). From the diameters (a and b) and the thickness of the slice (h) the volume of each slice was calculated as a cylinder with h for height and elliptical cross section (volume = $\pi h a b / 4$). After integrating the volumes for each weighted body part separately we used the actual weight measurement and assigned an individual density value for each body part for each fly and calculated the mass of each slice from the volume and density. We then found the

position of the center of mass of the fly on the long axis of the body by summing the moment of mass of each slice along the antero-posterior axis of the body and dividing it by body length. We assumed that the center of mass falls on the bilateral symmetry line of the body and that body length axis transects all body cross sections (slices) through their centroid. The MOI for rotation about the dorsoventral axis of the body (yaw) and about the long axis of the body (roll) where both axes pass through the center of mass of the body was calculated from the MOI of each slice about its three major axes passing through its centroid:

$$\begin{aligned} I_{xx} &= ma^2/16 + mh^2/3 \\ I_{yy} &= mb^2/16 + mh^2/3 \\ I_{zz} &= m(a^2 + b^2)/16 \end{aligned} \quad (1)$$

And the parallel axis theorem for displaced axis of rotation:

$$MOI_{\text{displaced}} = MOI_{\text{centroid}} + mR^2 \quad (2)$$

where m is the mass of the slice and I_{xx} is the MOI about diameter b , I_{yy} is the MOI about the diameter a and I_{zz} is the MOI about the slice thickness (h). R is the distance between the centroid of the slice to the axis of rotation running through the center of mass of the body and MOI_{centroid} is I_{xx} , I_{yy} , or I_{zz} depending on the relevant rotation. Finally, the MOI of all slices are summed to give the total MOI for the fly for a given rotation. During flight the front legs of *C. dalmanni* are positioned parallel to the long axis of the body. The mass of the massive front legs was added to the calculation of the MOI as a point mass assumed to be located at 15% of body length below the anterior edge of the thorax (Fig. 1b). The mass of the posterior legs was included in the mass of the thorax. Due to the tedious process, MOI was only measured from ten males and ten females. The flies for the MOI analysis were chosen to have body mass similar to the average measured from all the flies (mean body mass \pm SD $\delta = 7.00 \pm 0.499$, $\text{♀} = 6.96 \pm 0.353$ mg, $n = 10$ per sex.). The analysis was repeated once for the entire body and once just for the head about an axis running through the point of contact between the head and thorax. For the entire body MOI was also calculated for rotations in a horizontal plane about a vertical axis passing through the center of mass while the fly is oriented in the air with its long axis inclined to the horizontal at pitch angles $\chi = 10^\circ, 30^\circ, 50^\circ$ and 70° (Fig. 1c). In this analysis the MOI for $\chi = 0$ and 90° is equivalent, respectively, to the MOI for yaw and roll rotations about the morphological axes of the fly.

Free flight experiments

The free flight trajectories were tracked inside a rectangular flight chamber ($1.0 \times 0.7 \times 0.7$ m) made of four Plexiglas

walls covered from above by a tent-shaped mosquito net (Fig. 2a). The entire flight chamber was installed inside a walk-in temperature ($26 \pm 1.5^\circ\text{C}$) and humidity (RH = 50–75%) controlled chamber. The walls and floor of the enclosure were covered with a black background and the top covered by a dark curtain to prevent interference from outside of the chamber and to limit light within the chamber to a constant light level emitted by four clusters of white LEDs each including 16 LEDs (20° viewing angle, 18,000 mcd for each LED). The LED clusters were installed 60 cm above the center of the flight chamber in a rectangular configuration that provided uniform light within the center of the chamber where fly trajectories were tracked. Four near infrared (850 nm) arrays of 120 LEDs each, two from above and two from the sides, supplemented the light level and spectrum in the chamber and were used to identify the flies from the black background by the tracking system. The tracking system (Trackit, BIOBSERVE, Germany) uses two CCD cameras with overlapping views connected to a computer. The cameras were aimed at an angle of 50° to the horizon on opposite sides of the top of the chamber (80° relative to each other, 0.9 m apart). The system analyzes the two camera views to calculate the three dimensional positions of the centroid of the fly. The fly is tracked at an average frequency of 60 Hz, inside a $30 \times 30 \times 30$ cm pre-calibrated virtual sampling cube (see Fry et al. 2000 for a detailed explanation of the system, calibration and testing procedures). The sampling volume where flies were tracked was located at the center of the flight chamber 20 cm away from the nearest wall, and was elevated 5 cm above the floor of the chamber.

Either male or female flies were introduced into the chamber in groups of 10–12 and allowed to roam voluntarily within the chamber for 3–4 h. The flies mostly walked along the floor and walls of the chamber taking off to the air only occasionally. All tracked flights were treated as independent. To ensure individual variation within the sex groups we repeated the experiment with seven groups per sex using new (naïve) flies each time (total flies used $\text{♀} = 76$ and $\text{♂} = 76$).

Trajectory data analysis

The raw flight trajectory data obtained from the tracking system are the positions of the centroid of the fly along the orthogonal X , Y and Z axes of the sampling cube (Z is the vertical, positive values are up, right hand rule) and time (Fig. 2). We only analyzed flight trajectories that included data of more than 20 consecutive time points (flights longer than 0.33 s). The distance of the sampling volume from the floor and walls removed the possibility of tracking trajectories that are takeoffs. As a first step we needed to define

and separate turns from straight flight sections. In the second step (hereafter “turn performance”) we focused on the upper end of the observed turns and compared turn performance between the sexes. The raw data were re-sampled at 60 Hz using cubic-spline interpolation to correct for non-uniform sampling rate by the tracking system. Then a 5-point-average smoothing filter was applied on the data to remove random tracking errors and to ensure that only consistent deviations from straight horizontal flight would be identified as turns. The smoothed data were used to calculate the three orthogonal vector components of the 3D flight velocity from numerical time derivatives of the position data as in Rayner and Aldrige (1985). A second time derivative provided the accelerations. From the horizontal components of velocity and acceleration (along the X and Y axes) we calculated for each time point the instantaneous curvature (k_{xy}) of the projection of the trajectory on the horizontal plane.

$$k_{xy} = (u_x a_y - u_y a_x) / (u_x^2 + u_y^2)^{3/2} \quad (3)$$

where u represents velocity, a represents acceleration and the subscripts x , y indicate the direction along the two horizontal axes. Curvature is the inverse of the radius of

the trajectory. The two horizontal velocities (u_x , u_y) were used to calculate horizontal flight speed (U_{xy}) and direction from vector analysis and the calculated instantaneous flight directions were numerically derived with respect to time to yield the turn rate. We then defined sections in the turn rate data exceeding 250 deg s^{-1} as indicating a deviation from straight flight (Fig. 2c, d). Both left and right turns were treated equally by adjusting the sign of curvature and turn rate to positive values. In each of the sections identified as turns, the maximum point of the turn rate curve was identified and the time interval between the two neighboring minimum points was defined as the turn duration. Turn amplitude was defined as the difference in flight direction between the start and end of the turn. For each of the turns defined this way we calculated the mean turn rate, mean horizontal speed, and the mean turn path radius ($1/k_{xy}$) by averaging all data points within that turn. The technique resulted in 857 sections identified as turns (443 turns for males and 414 for females). We used these average parameters for a general description of the full range of turning behavior observed. The remainder of the data (straight flight sections) was saved to calculate flight speeds and turn frequency.

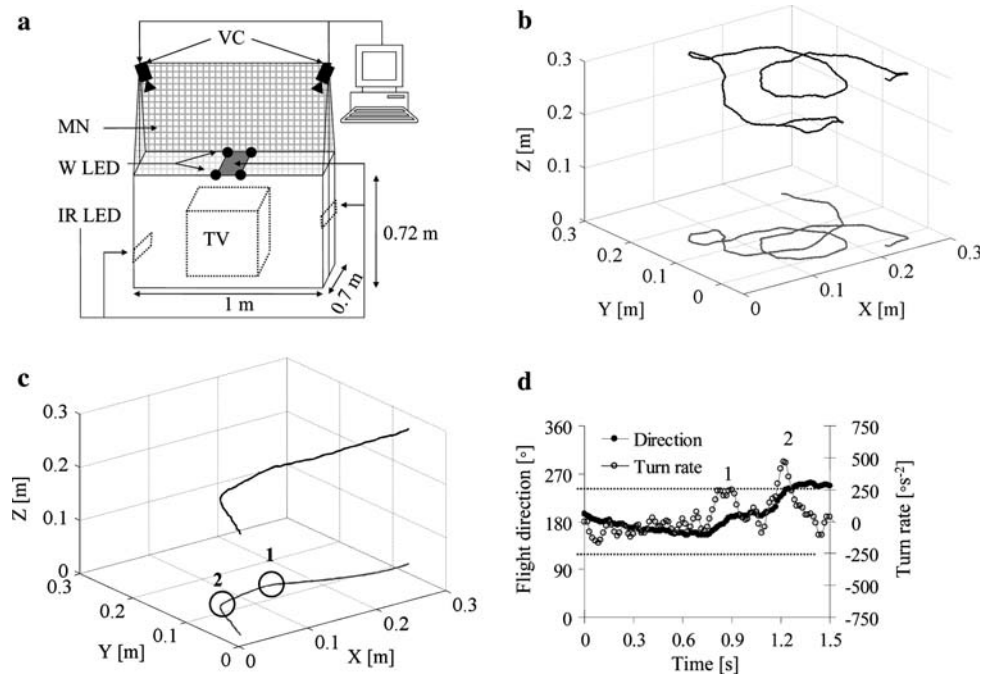


Fig. 2 **a** An illustration (not to scale) of the flight chamber and the tracking system. *VC* video cameras, *TV* tracking volume, *MN* mosquito net, *W LED* white LED clusters, *IR LED* near infrared LED clusters. **b** An example of a long flight trajectory data as tracked continuously for 15.73 s within the sampling volume of the flight chamber. The upper (black) line is the 3-dimensional trajectory data. The bottom (grey) line is the projection of the flight trajectory on the horizontal plane ($Z = 0$). **c** A short trajectory (1.58 s) showing two

sections (numbered circles) where the fly changed direction in the horizontal plane. **d** Time series of the direction and the turn rate of the same trajectory as in **c** demonstrating the cutoff value of turn definition in the analysis. Numbers of peaks in the turn rate graph refer to the circles in **c**. While the section in circle 1 is just below the cutoff turn rate (250 deg s^{-1} , dashed lines) and is therefore not considered a turn, maximum turn rate in circle 2 exceed the cutoff value and is therefore considered a turn

Comparison of turn performance

To test if males have reduced turning performance relative to females, we used a subset of the turns identified above. This was done for three reasons: (1) If drag, MOI or other factors limit turning performance we expected the limitation to be demonstrated as flies perform closer to their maximum, (2) we noted that when flies were flying very slowly or hovering, the calculation of flight direction and turn rate was subject to higher tracking error due to the calculation of angles (direction) from translations at a fixed time frequency, (3) the smoothing filter we used was useful in separating turns from straight sections but smoothed the turn data. Therefore, to compare turning performance we trimmed our data set to include only turns that had turn amplitude $>30^\circ$, had mean flight speed $> 2.5 \text{ cm s}^{-1}$ and a maximum turn rate $>350 \text{ deg s}^{-1}$. This resulted in a reduction of the data to 242 and 191 turns for female and males, respectively. For each one of these turns we went back to the raw (unsmoothed) data and within a 350 ms time window centered on the point of maximum turn rate we doubled the sampling frequency to 120 Hz using cubic-spline interpolation. The time point of maximum turn rate within each such time frame was assigned an adjusted time value of $t = 0$ and the turn duration was calculated as the interval in which turn rate was $>20\%$ of the maximum. We used the median of the remaining tails to calculate the flight direction prior to and after the turn and the turn amplitude. Turn path radius, turn rate, and horizontal speed were calculated as before but this time from the unsmoothed data. The turns obtained this way were more repeatable and had a higher time resolution which allowed us to calculate the second time derivative of flight direction and obtain the angular acceleration within the turn. We were interested in the angular acceleration because turns with similar average turn rates can result from different acceleration regimes and because we were interested to get an idea of the order of magnitude of torques required to rotate the body with the calculated MOI. The acceleration was divided into two sections based on its direction. In the first half of the turn (from the initiation of the turn to time point $t = 0$) the flies have an angular acceleration (α_1) and in the second half (from $t = 0$ to the end of turn) angular deceleration (α_2). After comparing turn performance between females and males using all the turns in the trimmed data set ($n = 433$ turns), we repeated the analysis only on turns from the upper quartile (25%) of turn rate of each sex within this subset. The upper quartile was chosen to represent the highest turn performance in the observed data while retaining reasonable sample size for statistical analysis ($\text{♀} = 60$ turns, $\text{♂} = 48$).

Statistical analysis

We used Analysis of Covariance (ANCOVA) with body mass as a covariate to compare morphology between males and females and used ANCOVA with flight speed and turn amplitude as covariates while comparing turning behavior. Interactions between the covariates and sex were only included in a general linear model (GLM) if they were significant. Except for the comparison of mass of different body parts (morphological analysis) all ANCOVA tests were performed on log transformed data. Non-dimensional parameters (moment of area, aspect ratio) and averages of the measured parameters were compared between sexes using the t test. Tests and calculation of adjusted mean were performed with STATISTICA (StatSoft Inc.) and SYSTAT (SYSTAT Software Inc.). Results are reported as mean ± 1 standard deviation (SD) in the text and tables. In the figures we report mean \pm standard error of the mean (SE) to ease evaluation of differences between the sexes.

Results

Morphological measurements

Mean morphological measurements for male and female *C. dalmanni* ($n = 20$ flies per sex) are presented in Table 1. Males and females did not differ significantly in body mass ($P = 0.376$). In an ANCOVA with body mass as a covariate, no inter-sex differences were found in the mass of the eyes or in the total mass of the head ($P > 0.73$). Relative to their body mass, the mass of the eye-stalks was bigger in males ($P \ll 0.001$) and the mass of the head minus eyes and eye-stalks was marginally larger in females ($P = 0.066$). Inspection of the adjusted mean (mean corrected for body mass) shows that the added mass of eye-stalks in males (0.034 mg) is almost matched by the added mass of the head without eye-stalks and eyes in females (0.028 mg), which explains why the total mass of the head did not differ between sexes. Males had larger thorax ($P < 0.045$) and front legs ($P < 0.001$) and females had larger abdomens ($P < 0.001$). Relative to the logarithm of body mass, log eye span of males was larger than in females ($P < 0.001$). The inter-sex difference amounted to an increase of 45.6% (2.6 mm) in males relative to the eye span of females. The estimated MOI of the head for roll and yaw in males were more than double the MOI of females ($P < 0.001$ in both cases). The MOI of the entire body for roll was higher 1.9-fold in males ($P < 0.001$) but the MOI of the entire body for yaw did not differ ($P = 0.088$). For rotation about a vertical axis when the fly's long axis is inclined at 70° with the horizontal the

MOI of the body of males was 1.49-fold higher than females ($P < 0.001$).

Males had longer wings ($P < 0.001$) and had a larger wing area ($P < 0.001$) relative to their body mass. As a result wing loading (body weight/wings area) for females was higher ($P < 0.001$) by 12% compared to males (8.3 ± 0.77 and $9.2 \pm 0.97 \text{ Nm}^{-2}$ for males and females, respectively). The second moment of wing area, a quantity that links aerodynamic force with wing area in flapping wings, was 22.4% larger in males relative to females ($P < 0.001$). The bigger wing of males did not differ in aspect ratio ($P > 0.14$), or the non dimensional radius of gyration ($P > 0.87$) from wings of females indicating that wing growth did not incur a change in wing shape.

Flight trajectories

A total of 406.2 and 386.5 s of flight from 249 and 267 flight trajectories were recorded from 76 female and 76 male flies, respectively. The average flight trajectory tracked lasted 1.630 ± 1.638 s for females and 1.445 ± 1.457 s for males. Out of the total tracked trajectories, 98 (39.3%) and 139 (52.1%) of the tracks of females and males, respectively, contained no turns as defined by our criteria. Turn frequency as calculated by dividing the total number of turns with total air time, was 1.15 and 1.02 turns s^{-1} for males and females, respectively. Using only the turns matching the stricter criteria of the turn performance analysis yielded 0.49 and 0.6 turns s^{-1} which corresponds to a 22% higher turning frequency in females.

Fig. 3 Flight speed of *C. dalmanni*. Frequency distribution of vertical (a, c) and horizontal (b, d) flight speeds for all the turns (a, b) and for the trajectories that did not include turns (c, d). During trajectories that did not include turns ($n = 237$) males had higher horizontal speed than females ($P < 0.048$). The vertical flight speed was faster ($P < 0.001$) and flies tended to loose height. During turns ($n = 857$) horizontal flight speed of females was faster than males ($P < 0.021$)

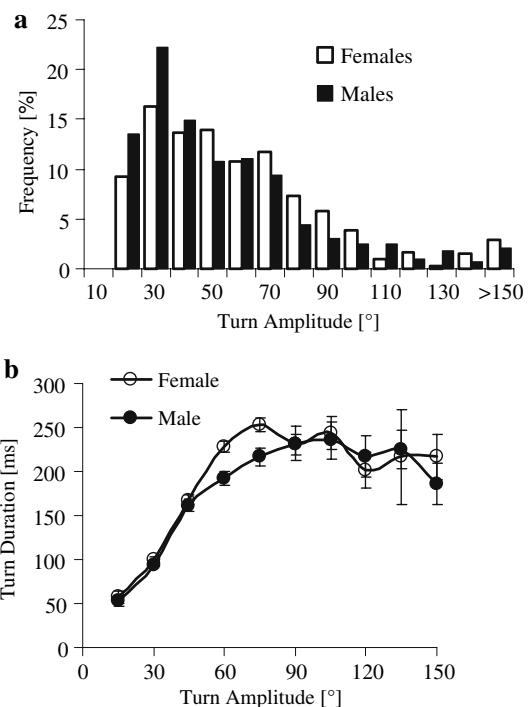
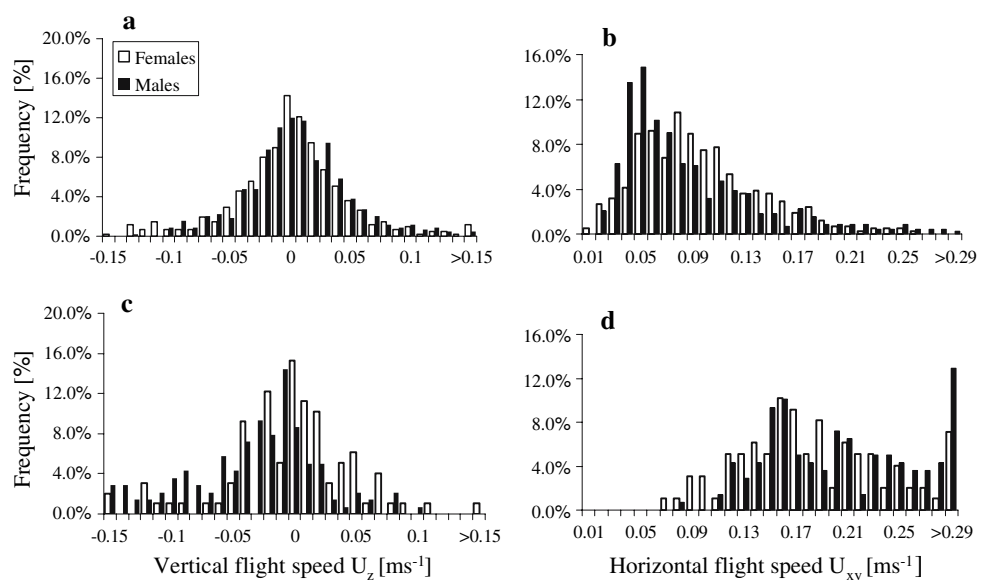
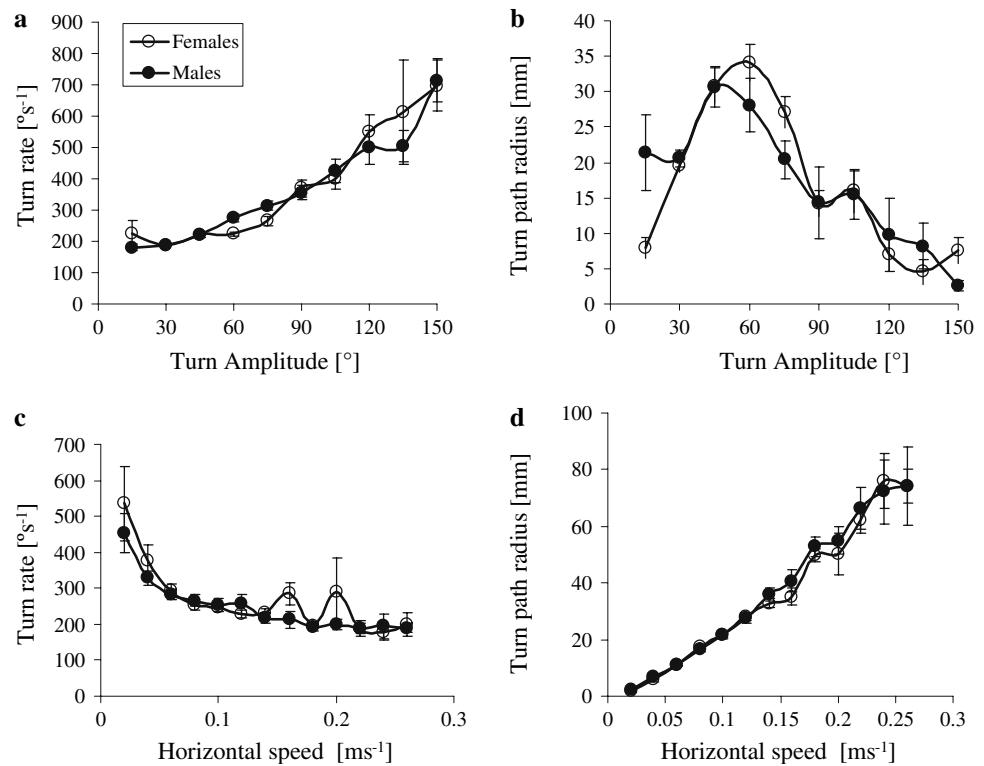


Fig. 4 Turn amplitude and turn duration in *C. dalmanni* during free flight (414 and 443 turns for female and males, respectively). **a** Histogram of turn amplitude frequency in males and females. **b** Turn duration increased with turn amplitude up to 90° and then remained relatively constant. The results are shown as averages of the data binned at 15° for males and females separately. Error bars are standard error of the mean

Flight speed

In straight trajectories (those that did not include turns), the mean 3D flight speed per track (Fig. 3) of males

Fig. 5 Mean turn rate (**a, c**) and mean turn path radius (**b, d**) in *C. dalmanni* during free flight. The plots are shown as averages \pm SE from data ($n = 857, 414$ and 443 turns for female and males, respectively) binned over 15° of turn amplitude (**a, b**) and 0.025 ms^{-1} of horizontal flight speed (**c, d**). Turn rate increased with turn amplitude but decreased with horizontal flight speed. Turn path radius increased with horizontal flight speed but decreased with turn amplitude at turns $>60^\circ$



($21.6 \pm 6.6 \text{ cm s}^{-1}$) was slightly but significantly (t test, $t_{235} = -2.3$; $P < 0.023$) higher than the flight speed of females. ($19.5 \pm 7.7 \text{ cm s}^{-1}$). A comparison of the mean vertical flight path angle (the flight direction measured relative to the horizontal plane) showed that females tended towards leveled flight ($-2.0^\circ \pm 1.70$) while males tended to loose altitude ($-10.2^\circ \pm 1.26$) ($t_{235} = 3.96$, $P < 0.001$). When the trajectories were arbitrarily divided into leveled ($-3^\circ < 0 < 3^\circ$), ascents ($>3^\circ$) and descents ($< -3^\circ$) based on the vertical flight angle no differences in horizontal flight speed between the three flight types (ANOVA, $F_{2,231} = 0.06$, $P = 0.94$) or between sexes ($F_{1,231} = 3.2$, $P > 0.075$) was found. The average horizontal flight speed in trajectories with turns ($\sigma = 9.4 \pm 6.2$, $\text{♀} = 10.7 \pm 5.5 \text{ cm s}^{-1}$) was approximately half the speed in trajectories without. When the average horizontal flight speed in the straight section prior to a turn was compared with the average speed during the turn an ANOVA (for repeated measurements) showed that both sexes slowed down during a turn ($F_{1,856} = 85.4$, $P < 0.001$) and females were flying faster than males ($F_{1,856} = 5.35$, $P < 0.021$). Post-hoc tests of the interaction ($F_{1,856} = 3.95$, $P < 0.047$) showed that the speed of females prior to the turn was the highest and the speed of males during the turn was the lowest (Tukey, $P < 0.001$ for both cases). The mean vertical speed during the turns ($n = 857$) was $0.1 \pm 4.7 \text{ cm s}^{-1}$. It did not differ between the sexes ($t_{813} = -0.8$, $P > 0.41$) and showed a symmetrical distribution around zero (Fig. 3).

Turn dynamics

Figure 4 shows that in both sexes turn duration increased rapidly with turn amplitude up to a turn size of 90° and then remained relatively unchanged at larger turns. Figure 5 shows the relationship of turn path radius and turn rate with turn amplitude and horizontal flight speed. Using all turns from both sexes ($n = 857$), turn rate was found to increase with turn amplitude ($r = 0.74$, $P < 0.001$) but showed a logarithmic decrease with horizontal flight speed ($r = 0.37$, $P < 0.001$). Turn path radius increased with horizontal flight speed ($r = 0.94$, $P < 0.001$) and decreased with turn amplitudes ($r = 0.264$, $P < 0.001$; after log transformation). Figure 6 shows the fine-scale time-line for turns that passed the criteria for the turn performance analysis. For these turns, mean turn amplitude did not differ between males and females ($P > 0.22$) and the average turn amplitude was $64^\circ \pm 26.8^\circ$. Turns are typically sharp spikes in the turn rate curve (Figs. 2, 6a). The maximum point depends on the turn amplitude but the rapid change in turn rate occurs over a fairly constant duration ($\sim 160 \text{ ms}$). Immediately following the sharp increase in turn rate there is a sharp decrease. This is registered as two accelerations with opposing sign in the angular acceleration curve (Fig. 6b). The relation between maximum turn rate and turn amplitude over a relatively fixed turn duration results in larger accelerations for larger turn magnitude that peak (in the order of magnitude of 10^4 s^{-2}) 33 ms before and after the maximum turn rate.

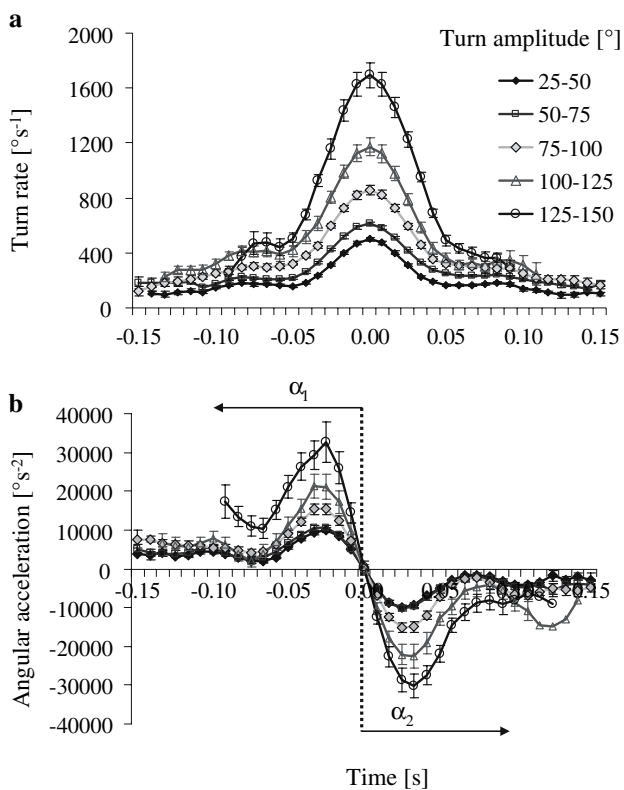


Fig. 6 The time line of turn rate (**a**) and angular accelerations (**b**) of *C. dalmanni* during aerial turns. Only data for turns used to assess turn performance ($n = 433$) are shown (see text). The figures show averages (\pm SE) of the pooled data from both sexes binned at 25° of turn amplitude. The time axis is centered at $t = 0$ for the point of maximum turn rate. Turns are rapid increases in turn rate with the maximum turn rate correlated with turn amplitude. The turns are made of two opposite angular accelerations one for the initiation (α_1) and one for the termination of the turn (α_2)

Turn performance

Table 2 summarizes the mean of turn parameters observed from both sexes. During free flight (all turns observed) the mean turn amplitude was larger in females ($P < 0.033$) but so was the mean turn duration ($P < 0.001$). The mean of turn rate and turn path radius did not differ between the sexes. When only the turns that passed the criteria for the turn performance test or only the upper quartile of that turns were compared between the sexes only turn duration differed ($P < 0.001$; upper quartile $P < 0.004$) with females having slightly longer turn durations.

To specifically test whether male flies have reduced turning capabilities compared to females, we compared turn duration between the sexes for a given turn amplitude and compared turn rate and turn path radius for a given turn amplitude and horizontal flight speed in an ANCOVA. The results are summarized in Table 3 as the adjusted means. For a given turn magnitude, turn duration was still higher in females than in males ($P < 0.001$; upper quartile

$P < 0.026$). For a given turn amplitude and horizontal flight speed males had smaller turn path radius ($P < 0.027$) and higher turn rate ($P < 0.039$) than females. When only the upper quartile of turn rate of the data were analyzed in the same ANCOVA turn path radius no longer differed between the sexes ($P < 0.17$) but the difference in turn rate was persistent ($P < 0.047$).

Angular accelerations of the turns reached values as high as $5 \times 10^4 \text{ s}^{-2}$ in the turns with the highest turn rate (Fig. 7). No difference in the first angular acceleration (α_1) was found between the sexes after correcting for turn rate ($P > 0.26$; upper quartile $P < 0.45$). The second angular acceleration (α_2) was larger in males ($P < 0.02$; upper quartile $P < 0.029$).

Discussion

Our analysis provides a first exploration to the aerial turning behavior of stalk-eyed flies. The flight of *C. dalmanni* is slow and sluggish, and previous studies have speculated that longer eye-stalks result in reduced flight performance (Swallow et al. 2000). Since modifications in head morphology results in changes to the MOI but not in changes to the mass of the head or body, we hypothesized that if eye-stalks become a limitation to flight this will be most evident during aerial maneuvers which include rapid rotations of the body. When comparing the free flight turning behavior of males and females we found that females tended to make larger turns more frequently than males and flew faster while turning. However, for a given turn amplitude and flight speed both sexes performed similarly with males slightly outperforming females. The observed differences in turning parameters were in general very small with a large overlap between the sexes in all the parameters tested. Therefore the emerging overall image from this study is that the statistical differences in turning performance are probably of minor ecological significance and males and females perform very similarly in the range of turns tested. This suggests that if males have any mechanical handicap stemming from longer eye-stalks then they were capable of compensating for it in our experiment. Such compensation likely occurs through wing-beat kinematics and/or morphological design of the flight apparatus.

Limitations of an analysis based on flight tracks

While interpreting the results of this study it is useful to first consider its limitations and assumptions. First, our tracking system operated at 60 Hz which implies a time resolution of 16.7 ms between successive data points. This means that fast events such as low amplitude turns that last less than 50 ms (Fig. 4b) would be represented by only three data points. To prevent this we limited our analysis to

Table 2 Mean ± SD of turning parameters for male and female *C. dalmanni* as measured during free flight

Parameter measured	♀	♂	Significance test
All turns	<i>n</i> = 414	<i>n</i> = 443	
Turn duration (ms)	186 ± 81.8	158 ± 80.9	<i>t</i> ₈₅₅ = 5.27***
Turn amplitude (°)	54 ± 31.4	49 ± 36.2	<i>t</i> ₈₅₀ = 2.14*
Turn path radius (mm)	24 ± 19.0	22 ± 22.5	<i>t</i> ₈₄₆ = 1.10
Turn rate (deg s ⁻¹)	270 ± 155.0	271 ± 149.5	<i>t</i> ₈₅₅ = -0.09
Horizontal speed (cm s ⁻¹)	9.4 ± 5.45	8.4 ± 6.17	<i>t</i> ₈₅₂ = 2.58**
Turn performance	<i>n</i> = 242	<i>n</i> = 191	
Turn duration (ms)	173 ± 48.1	157 ± 50.0	<i>t</i> ₄₃₁ = 3.60***
Turn amplitude (°)	65 ± 26.6	62 ± 27.1	<i>t</i> ₄₃₁ = 1.21
Turn path radius (mm)	18.7 ± 13.88	18.8 ± 18.56	<i>t</i> ₄₃₁ = -0.02
Turn rate (deg s ⁻¹)	402 ± 221.9	428 ± 226.0	<i>t</i> ₄₃₁ = -1.20
Horizontal speed (cm s ⁻¹)	10.8 ± 5.19	10.4 ± 6.50	<i>t</i> ₄₃₁ = 0.71
4th quartile ω	<i>n</i> = 60	<i>n</i> = 48	
Turn duration (ms)	142 ± 38.1	122 ± 34.0	<i>t</i> ₁₀₆ = 2.9***
Turn amplitude (°)	92 ± 33.5	86 ± 33.4	<i>t</i> ₁₀₆ = 0.88
Turn path radius (mm)	6 ± 3	5 ± 3	<i>t</i> ₁₀₆ = 1.80
Turn rate (deg s ⁻¹)	685 ± 282.6	733 ± 235.3	<i>t</i> ₁₀₆ = -0.94
Horizontal speed (cm s ⁻¹)	7.3 ± 3.3	6.3 ± 3.0	<i>t</i> ₁₀₆ = 1.67

U_{xy} denotes horizontal speed ω denotes turn rate

Asterisks denote significance of differences between the mean * *P* < 0.05; ** *P* < 0.01; *** *P* < 0.001

Table 3 Adjusted mean for turn duration, turn path radius (*r*), turn rate (ω) and angular accelerations (α₁, α₂) as calculated from an ANCOVA using the specified covariates

Parameter tested	♀	♂	Covariate	Significance test
Turn performance	<i>n</i> = 242	<i>n</i> = 191		
Duration (ms)	165.6	149.5	Amp	<i>F</i> _{1,430} = 11.7***
Mean <i>r</i> (mm)	13.1	12.3	Amp, <i>U_{xy}</i>	<i>F</i> _{1,429} = 4.95*
Mean ω (deg s ⁻¹)	363.9	383.1	Amp, <i>U_{xy}</i>	<i>F</i> _{1,429} = 4.28*
Mean α ₁ (deg s ⁻²)	6,967.2	7,308.9	Max ω	<i>F</i> _{1,430} = 1.30
Mean α ₂ (deg s ⁻²)	6,310	6,839	Max ω	<i>F</i> _{1,430} = 5.45*
4th quartile (ω)	<i>n</i> = 60	<i>n</i> = 48		
Duration (ms)	135	119	Amp	<i>F</i> _{1,105} = 5.08**
Mean <i>r</i> (mm)	4.5	4.0	Amp, <i>U_{xy}</i>	<i>F</i> _{1,104} = 1.09
Mean ω (deg s ⁻¹)	639.5	705.7	Amp, <i>U_{xy}</i>	<i>F</i> _{1,104} = 4.04*
Mean α ₁ (deg s ⁻²)	15,148	15,014	Max ω	<i>F</i> _{1,105} = 0.58
Mean α ₂ (deg s ⁻²)	13,589	16,765	Max ω	<i>F</i> _{1,105} = 4.88**

Amp is the turn amplitude, *U_{xy}* is the horizontal flight speed

Asterisks denote significant differences between the sexes * *P* < 0.05; ** *P* < 0.01; *** *P* < 0.001

turns with amplitude greater than 30°. Turns with larger amplitude involved higher turn rates (Figs. 5, 6). At turn amplitude of 150° and turn duration of 200 ms the average angular resolution would be 12.5° per time step. If we assume this (±12.5°) to be the maximum error for tracking turn amplitude, the error is in most cases higher than the

difference observed between the means of both sexes (Table 2). Similarly the time resolution (±16.7 ms) is roughly the same as the differences observed between the mean of both sexes in turn duration. Therefore the small differences we observed in turn duration are within the error range of the tracking system and should be treated

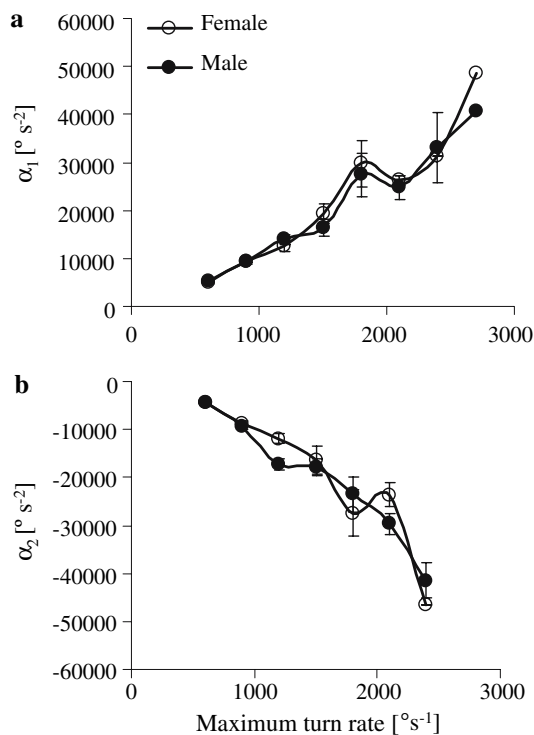


Fig. 7 The mean angular accelerations (**a**) and deceleration (**b**) measured during aerial turns of *C. dalmanni* as a function of maximum turn rate. Only data used to assess turn performance ($n = 433$) are shown (see text). Symbols are average accelerations (\pm SE) binned at 300 deg s⁻¹ of maximum turn rate

with caution. The system is therefore adequate to describe the low flight speed and weak turning performance of *C. dalmanni* but may be inadequate to pick up small differences in turning performance between the sexes. Whether differences smaller than 12.5° in turn amplitude and 16.7 ms in turn duration are of biological importance may be debated. Second, the tracking system only tracked the centroid of the fly without providing data on orientation of the body. In the following paragraphs we discuss the consequence of eye-span length on rotation of the body in air and it is important to remember that flight trajectory data is only relevant to this discussion if the fly orients its body during the turn so that the projection of its body length on the horizontal plane has the same angle as the horizontal flight direction. Several fly species are capable of sideways movements without rotating the body and this behavior is typically associated with visually tracking moving targets (Wagner 1986; Land and Collett 1974; Collett and Land 1975). The assumption that the flies rotate their body with flight direction is therefore more justified for goal oriented flight through a stationary background (Wagner 1986). Third, to improve the tracking accuracy of the system and to prevent changes to flight behavior that are due to visual perception of the background we used a dark background in our experiments. Visual conditions

have been shown to influence flight behavior in flies that rely on vision for flight control (e.g. Wagner 1986). Since we were mostly concerned with mechanical rather than sensory effects and compared turn parameters of males against the same turns performed by females in the same flight chamber this should not be a major limitation here. However, while comparing our data to previous studies (see below) we can not rule out the possibility that the flies might behave differently in different visual settings. Fourth, our analysis compares the flight performance during voluntary free-flight and there is always the possibility that the flies were not performing close to their maximum capabilities. A limitation to flight performance would be expected to be more pronounced closer to maximum performance. Some support that the flies were close to their maximum performance can be interpreted from the fact that they increased their turning path radius with flight speed (Fig. 5d) and slowed down flight speed during the turns (Fig. 3). This can imply that the flies were incapable of generating a larger centripetal force while turning. To further insure that we were measuring higher-end performance we trimmed our data set of the total turns observed to the upper ~50% (“turn performance”) and then to the upper quartile of that subset. Finally, our analysis is focused on mechanical constraints that may emerge during aerial turns from possessing long eye-stalks. Eye-stalks length may have additional adaptive or maladaptive consequences that are not directly related to flight mechanics (e.g. increased binocular visual capabilities see Burkhardt and de la Motte 1983, reduced spatial resolution see Buschbeck and Hoy 1998). These are not discussed here.

Implication of the inter-sex differences in the MOI

Differences in the distribution of mass along the body’s major axes can affect turning performance through

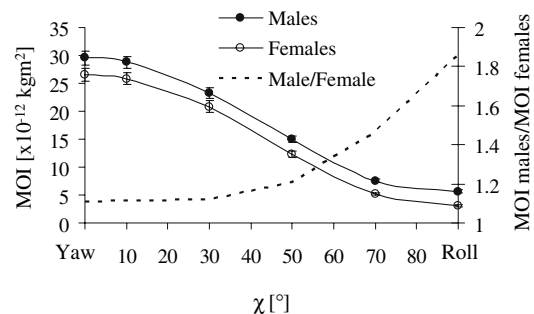


Fig. 8 The calculated MOI of both sexes for the rotation in a horizontal plane as a function of body angle (χ) during flight. MOI is calculated for a vertical axis (see Fig. 1c and text). For $\chi = 0^\circ$ the MOI is the MOI for yaw and for $\chi = 90^\circ$ the MOI is the MOI for roll. The dashed line is the ratio between the calculated MOI of males and females

changes to the MOI. The turns analyzed here are changes in flight direction in the horizontal plane. If the flight paths of the flies are any indication of their orientation in space (i.e. the flies rotate their body to align it with the flight direction) then the measured turn rate is an indicator of the angular velocity and acceleration of body rotations about a vertical axis. During slow flight the long axis of the body is tilted at a large angle with the horizontal as in “normal hovering” described by Weis-Fogh (1973). Thus, for the type of turns analyzed here, the functional axis of rotation in the horizontal plane can be viewed as a vertical line passing through the center of mass while the body is pitched by an angle (χ) at its flight posture (Fig. 1b, c). Figure 8 shows how the calculated MOI of the flies for rotation about a vertical axis changes with different values of χ . MOI is the highest for yaw, ($\chi = 0^\circ$), and the difference between the two sexes is small in proportion to the overall MOI of the body. MOI continues to decrease as χ increases, to the level of the MOI calculated for roll about the body’s longitudinal axis at $\chi = 90^\circ$. In the process, although the difference between the sexes that is due to lateral expansion of the eyes is maintained fairly constant, the proportion to the total MOI of the body increases (Fig. 8). During slow flight or hovering the body angle of *C. dalmanni*, as estimated from observing the flies in their cages, is close to 70° relative to the horizontal (Fig. 1b). At this body angle the MOI of male flies is 1.49-fold higher than the MOI of females and the absolute difference is $2.5 \times 10^{-12} \text{ kg m}^2$ (Table 1). Since our turning performance trials indicated no detectable difference in turning dynamics between males and females, males are expected to produce larger torques compared to females in order to achieve the exact same angular acceleration while rotating the body. Solely from MOI considerations (overlooking the additional effect of air resistant) and assuming a body angle of $\chi = 70^\circ$ the torques required are 1.49-fold of that required by females with the same body angle. Because air resistance adds additional complication to this scenario, it is difficult to estimate the exact compensation required by the males. At body lengths (and male eye span) smaller than 9 mm and maximal speeds of 0.3 ms^{-1} The Reynolds number for the body are typically <180 . Since body angle is close to vertical, the overall change to the effective area of the flies from having longer eye-stalks is probably small (Fig. 1). The eyes of males would have higher tangential speed while rotating at the same angular speed as a female but the somewhat higher drag of male eye-stalks might be offset to some extent by the larger abdomen of females (Table 1; Fig. 1). Since the flies slow down considerably during turning, drag due to eye span elongation may be a more important consideration for flight performance during fast straight flight.

Schilstra and van Hateren (1998) reported on head rotations relative to the thorax in blowflies during aerial turning. Other fly species rotate their entire body as one unit (Land 1999). During walking, stalk-eyed flies perform head saccades (Land and Nilsson 2002) but it is unknown if they do the same during flight. Our morphological analysis shows that for an assumed body angle $\chi = 70^\circ$ the difference in MOI between the sexes is mostly due to the change in head morphology. Rotations of the head relative to the thorax may have a slight effect on the MOI of the entire body especially if the head is rolled relative to the thorax so that the eye-stalks become parallel to the axis of rotation of the body. Simple observation of the flies turning in air does not support this idea, at least not to an extent that would be visible by the human eye.

Flight performance

Both male and female *C. dalmanni* have considerably elongated eye-stalks (Fig. 1; Table 1). By evaluating the effect of eye-stalks on flight performance through the comparison between the sexes we may be diminishing the effect of eye span length on turning performance compared to a similarly sized fly with no eye-stalks. Both sexes of *C. dalmanni* displayed aerial turns that are comparable to previously described aerial turns of other fly species (fruit fly: Mayer et al. 1988; Tammero and Dickinson 2002a; Bender and Dickinson 2006a; hoverfly: Collett and Land 1975; blowflies: Schilstra and van Hateren 1999; house fly: Wagner 1986). Our findings corroborate previous reports on an increase in turn duration with turn amplitude up to a certain point and then a leveling of the turn duration to roughly constant values (Fig. 4b; Mayer et al. 1988; Schilstra and van Hateren 1999). Also, the relation between turn rate and turn amplitude has been previously reported in several studies (Bender and Dickinson 2006a; Schilstra and van Hateren 1999; Mayer et al. 1988). Of particular use in comparing the turning performance of *C. dalmanni* to other flies are the studies on the aerial turns of blowflies (Schilstra and van Hateren 1999) and fruit flies (Fry et al. 2003). These studies report on the dynamics of aerial turns performed during free-flight. The 100 mg blowfly and the $<1.3 \text{ mg}$ fruit fly had reported maximum turn rates (yaw) close to $2,000 \text{ deg s}^{-1}$ and peak angular accelerations of approximately 10^5 deg s^{-2} for turn amplitude of 90° . For turns with a similar range of amplitude (75° – 100°), *C. dalmanni* with an intermediate body mass of 7 mg, reached, on average, a maximum turn rate of $860 \pm 296 \text{ deg s}^{-1}$ and the peak angular acceleration (α_1) averaged $1.5 \times 10^4 \pm 1.34 \times 10^4 \text{ deg s}^{-2}$ (Fig. 6). Turn duration reported in the above mentioned studies was 40 ms for the fruit fly and slightly less for the blowflies.

Table 2 shows that in the upper quartile of turn rate where turn amplitude averaged at 86° – 92° turn duration of *C. dalmanni* was on average 122 and 142 ms in males and females, respectively. Thus, although *C. dalmanni* displayed similar characteristics of turning behavior, the turning performance of both sexes of this species was to a great extent inferior to the turning performance observed in blowflies and fruit flies.

Even compared to reports from other members of the family Diopsidae, *C. dalmanni* emerges as a slow flyer rarely exceeding a horizontal flight speed of 0.3 ms^{-1} (Fig. 3). This upper value from our experiment is close to the average horizontal speed reported by Swallow et al. (2000) for *C. whiteii* and *C. quinqueguttata*, which are closely related to *C. dalmanni* and have similar body mass. Apart from inter-species differences, the difference in the observed flight speeds may relate to a different visual background (white) but also to the nature of flights analyzed. In our free flight experiments flies were flying voluntarily and we used only relatively long trajectories measured while the flies were airborne and maneuvering. Swallow et al. (2000) used shorter sequences, in a smaller volume, immediately after takeoff. Thus, it is likely that the short trajectories in that study represent bursts of fast flight during takeoff.

Dimorphism of the flight apparatus

The tracking system used in this study diminishes each fly into a point mass in space so that we can not evaluate changes in wingbeat kinematics between males and females in this study. Therefore, a full mechanistic explanation of how males compensate for higher MOI is beyond the scope and capabilities of this report. However, an interesting observation in this study is that apart from the obvious differences in eye-stalks and the larger abdomen of female flies (possibly due to the larger gonads), most of the morphological differences between the sexes can be classified as changes to the locomotion apparatus. The wing, thorax and front legs were all bigger in males. The front legs of male stalk-eyed flies function in terrestrial ritual fights (Panhuis and Wilkinson 1999) but also support and rotate the body while walking (G. Ribak, unpublished data). The wings and the flight muscle in the thorax power flight. It therefore seems that the increase in eye-stalk length in male *C. dalmanni* compared to females is correlated with an increase in the magnitude of the walking and flying apparatus. Swallow et al. (2000) reported that the thorax of males *C. whitei*, a dimorphic species of stalk-eyed fly, was larger than in females and larger than both male and female *C. quinqueguttata*, a closely related monomorphic species with

short eye-stalks. Furthermore, within *C. whitei*, wing length was longer in males than in females, and wing length was longer in the dimorphic *C. whitei* than in the monomorphic *C. quinqueguttata*. The current study further shows that wing shape (as described by the non-dimensional aspect ratio and radius of gyration) is the same in both sexes of *C. dalmanni* indicating that size and not shape is the main difference between the wings of males and females of equal body mass.

Marden (1987) found that the proportion of flight muscle mass to body mass correlates with maximum mass specific lift in insects that flap their wings conventionally (as oppose to clap-and-fling). Using thorax mass as a proxy for flight muscle mass we can conclude that the proportion of flight muscle in *C. dalmanni* is <0.4 and 0.33 in males and females, respectively (Table 1). For this range maximum lift according to Fig. 1 in Marden (1987) is in the order of 1.5–2.0 folds the body weight. If the inter-sex difference in thorax mass is indicative of a larger proportion of flight muscle mass in males this would support the idea that males can compensate and outperform females.

The small difference in wing length observed between the sexes (5%, Table 1) becomes somewhat bigger when considering total wing area (8.5%) and even bigger still when comparing the second moment of area of the wing (22.4%). The latter represents an estimate to the increase in aerodynamic force associated with an increase in size of a flapping wing. The aerodynamic force of a fixed wing scales linearly with wing area when wing shape is conserved. However, for a flapping wing, aerodynamic force scales non-linearly with wing length and area (Weis-Fogh 1973). The 22.4% difference in the second moment of area implies that in a hypothetical scenario in which male and female wings are flapped with exactly the same kinematics (amplitude, frequency and orientation) the simplest quasi-steady flow equations predict a 22.4% increase in average aerodynamic force (Weis-Fogh 1973). Since torque is a product of a moment arm and force, increased wings can generate larger torques either by producing larger forces or having a larger moment arm. Since it is currently unknown how males and females *C. dalmanni* beat their wings during aerial turning the adaptive potential of larger wings as a compensation mechanism for elevated MOI in males is still unclear and warrants further investigation.

Acknowledgments The authors are grateful for the help provided by G. S. Wilkinson in establishing *C. dalmanni* population in our lab. S. N. Fry helped in configuration and troubleshooting of the tracking system. D. Jolkowski, A. Egge, H. Moline, and T. Eviatar-Ribak helped in fly care and in the experiments. We thank Y. Brant for discussions on statistical analysis. The work was funded by NSF-grant No. IOB0448060.

References

- Alighali MA (1984) Mating and ovipositional behavior of the stalk-eyed fly *Diopsis macrophthalmia* on rice. *Entomol Exp Appl* 36:151–157
- Baker RH, Wilkinson GS (2001) Phylogenetic analysis of sexual dimorphism and eye-span allometry in stalk-eyed flies (Diopsidae). *Evolution* 55:1373–1385
- Bender JA, Dickinson MH (2006a) Visual stimulation of saccades in magnetically tethered *Drosophila*. *J Exp Biol* 209:3170–3182
- Bender JA, Dickinson MH (2006b) A comparison of visual and haltere-mediated feedback in the control of body saccades in *Drosophila melanogaster*. *J Exp Biol* 209:4597–4606
- Burkhardt D, de la Motte I (1983) How stalk-eyed flies eye stalk-eyed flies: observation and measurements of the eyes of *Cyrtodiopsis whitei* (Diopsidae, Diptera). *J Comp Physiol A* 151:407–421
- Burkhardt D, de la Motte I (1988) Big “antlers” are favored: female choice in stalk-eyed flies (Diptera, Insecta), field collected harems and laboratory experiments. *J Comp Physiol A* 162:649–652
- Buschbeck EK, Hoy RR (1998) Visual system of the stalk-eyed fly, *Cyrtodiopsis quinqueguttata* (Diopsidae, Diptera): an anatomical investigation of unusual eyes. *J Neurobiol* 37:449–468
- Christianson SJ, Swallow JG, Wilkinson GS (2005) Rapid evolution of postzygotic reproductive isolation in stalk-eyed flies. *Evolution* 59:849–857
- Collett TS, Land MF (1975) Visual control of flight behaviour in the hoverfly *Syrirta pipiens* L. *J Comp Physiol A* 99:1–66
- Cotton S, Fowler K, Pomiankowski A (2004) Condition dependence of sexual ornament size and variation in the stalk-eyed flies *Cyrtodiopsis dalmanni* (Diptera: Diopsidae). *Evolution* 58:1038–1046
- David P, Bjorksten T, Fowler K, Pomiankowski A (2000) Condition dependent signaling of genetic variation in stalk-eyed flies. *Nature* 406:186–188
- Dickinson MH (2005) The initiation and control of rapid flight maneuvers in fruit flies. *Integr Comp Biol* 45:274–281
- Dudley R (2002) Mechanisms and implications of animal flight maneuverability. *Integr Comp Biol* 42:135–140
- Ellington CP (1984) The aerodynamics of hovering insect flight II. Morphological parameters. *Philos Trans R Soc Lond B* 305:17–40
- Fox EA (1967) *Mechanics*. Harper & Row, NY
- Fry SN, Bichsel M, Muller P, Robert D (2000) Tracking of flying insects using pan-tilt cameras. *J Neuro Sci Methods* 101:59–67
- Fry SN, Sayaman R, Dickinson MH (2003) The aerodynamics of free-flight maneuvers in *Drosophila*. *Science* 300:495–498
- Frye MA, Tarsitano M, Dickinson MH (2003) Odor localization requires visual feedback during free flight in *Drosophila melanogaster*. *J Exp Biol* 206:843–855
- Götz KG, Wandel U (1984) Optomotor control of the force of flight in *Drosophila* and *Musca*. *Biol Cyber* 51:135–139
- Heide G, Götz GK (1996) Optomotor control of course and altitude in *Drosophila melanogaster* is correlated with distinct activities of at least three pairs of flight steering muscles. *J Exp Biol* 199:1711–1726
- Heisenberg M, Wolf R (1979) On the fine structure of yaw torque in visual flight orientation of *Drosophila melanogaster*. *J Comp Physiol A* 130:113–130
- Knell RJ, Fruhauf N, Norris KA (1999) Conditional expression of a sexually selected trait in the stalk-eyed fly *Diasemopsis aethiopica*. *Ecol Entomol* 24:323–328
- Land MF (1999) Motion and vision: why animals move their eyes. *J Comp Physiol A* 185:341–352
- Land MF, Collett TS (1974) Chasing behaviour of houseflies (*Fannia canicularis*). *J Comp Physiol A* 89:331–357
- Land MF, Nilsson D-E (2002) *Animal eyes*. Oxford University Press, New York
- Marden JH (1987) Maximum lift production during takeoff in flying animals. *J Exp Biol* 130:235–258
- Mayer M, Vogtmann K, Bausenwein B, Wolf R, Heisenberg M (1988) Flight control during “free yaw turns” in *Drosophila melanogaster*. *J Comp Physiol A* 163:389–399
- Panhuis TM, Wilkinson GS (1999) Exaggerated male eye span influences contest outcome in stalk eyed flies (Diopsidae). *Behav Ecol Sociobiol* 46:221–227
- Rayner JMV, Aldridge HDJ (1985) Three-dimensional reconstruction of animal flight paths and the turning flight of microchiropteran bats. *J Exp Biol* 118:247–265
- Reguera P, Pomiankowski A, Fowler K, Chapman T (2004) Low cost of reproduction in female stalk-eyed flies, *Cyrtodiopsis dalmanni*. *J Insect Physiol* 50:103–108
- Schilstra C, van Hateren JH (1999) Blowfly flight and optic flow. I. Thorax kinematics and flight dynamics. *J Exp Biol* 202:1481–1490
- Schilstra C, Van Hateren JH (1998) Stabilizing gaze in flying blowflies. *Nature* 395:654
- Shilito FJ (1971) Dimorphism in flies with stalked eyes. *Zool J Linn Soc* 50:297–305
- Swallow JG, Wilkinson GS, Marden JH (2000) Aerial performance of stalk-eyed flies that differ in eye span. *J Comp Physiol B* 170:481–487
- Swallow JG, Wallace LE, Christianson SJ, Johns PM, Wilkinson GS (2005) Genetic divergence does not predict change in ornament expression among populations of stalk-eyed flies. *Mol Ecol* 14:3787–3800
- Tammero LF, Dickinson MH (2002a) The influence of visual landscape on the free flight behavior of the fruit fly *Drosophila melanogaster*. *J Exp Biol* 205:327–343
- Tammero LF, Dickinson MH (2002b) Collision-avoidance and landing responses are mediated by separate pathways in the fruit fly, *Drosophila melanogaster*. *J Exp Biol* 205:2785–2798
- Wagner H (1986) Flight performance and visual control of flight of the free flying housefly (*Musca domestica* L.) III. Interaction between angular movements induced by wide and small field stimuli. *Philos Trans R Soc Lond B* 312:581–595
- Weis-Fogh T (1973) Quick estimates of flight fitness in hovering animals, including novel mechanisms for lift production. *J Exp Biol* 59:169–230
- Wilkinson GS (1993) Artificial sexual selection alters allometry in the stalk-eyed fly *Cyrtodiopsis dalmanni* (Diptera: Diopsidae). *Genet Res Camb* 62:213–222
- Wilkinson GS, Dobson GN (1997) Function and evolution of antlers and eye stalks in flies. In: Choe J, Crespi B (eds) *The evolution of mating systems in insects and arachnids*. Cambridge University Press, New York, pp 310–328
- Wilkinson GS, Reillo PR (1994) Female choice response to artificial selection on an exaggerated male trait in a stalk-eyed fly. *Proc R Soc Lond B* 255:1–6
- Wilkinson GS., Kahler H, Baker RH (1998) Evolution of female mating preference in stalk-eyed flies. *Behav Ecol* 9:525–533
- Wilkinson GS, Swallow JG, Christensen SJ, Madden K (2003) Phylogeography of sex ratio and multiple mating in stalk-eyed flies from Southeast Asia. *Genetica* 117:37–46
- Wright TF, Johns PM, Walters JR, Lerner AP, Swallow JG, Wilkinson GS (2004) Microsatellite variation among divergent populations of stalk-eyed flies, genus *Cyrtodiopsis*. *Genet Res Camb* 84:27–40
- Zeil J (1983) Sexual dimorphism in the visual system of flies: the divided brain of male Bibionidae (Diptera). *Cell Tissue Res* 229:591–610